Iranian Journal of Numerical Analysis and Optimization
Vol. 15, No. 2, 2025, pp 457–474
https://doi.org/10.22067/ijnao.2024.89654.1503
https://ijnao.um.ac.ir/

Research Article

Solving mixed singular integro-differential equation (IDE) using the finite elements method

M. Erfanian*, H. Zeidabadi and M.S. Hussein

Abstract

In this work, we describe a new method for the calculation of the numerical solution of the mixed singular integro-differential equation. The method is mainly based on a finite element approximation. For this purpose, we obtain the variational form of the problem under consideration. The resulting system has been approximated numerically by linear B-spline function. The method of convergence and its order of convergence are established.

*Corresponding author

Received 31 August 2024; revised 12 December 2024; accepted 25 December 2024

Majid Erfanian
Department of Science, School of Mathematical Sciences,University of Zabol, Zabol, Iran. e-mail: erfaniyan@uoz.ac.ir

Hamed Zeidabadi
Department of Applied Mathematics, Faculty of Mathematics and Computer Sciences, Hakim Sabzevari University, Sabzevar, Iran. e-mail: h.zeidabadi@yahoo.com

M.S. Hussein
Department of Mathematics College of Science University of Baghdad. e-mail: mmmsh@sc.uobaghdad.edu.iq

How to cite this article
Erfanian, M., Zeidabadi, H. and Hussein, M.S., Solving mixed singular integro-differential equation (IDE) using the finite elements method. *Iran. J. Numer. Anal. Optim.*, 2025; 15(2): 457-474. https://doi.org/10.22067/ijnao.2024.89654.1503

Finally, to investigate the accuracy of the proposed method some test examples are presented. The numerically obtained results are compared with another method for the validity of our results and shown by some tables and figures.

AMS subject classifications (2020): 65L60,44A45, 45B05, 65R20.

Keywords: Singular integro-differential equation; finite element approximation; Convergence; Error analysis.

1 Introduction

The integro-differential equation is a sophisticated mathematical construct that blends the principles of integral and differential calculus, serving as a vital tool in various fields such as physics, engineering, and applied mathematics. Need to write an introduction here singular integro-differential equations (SIDEs) appear in a lot of science, for example, in applied sciences, electromagnetics, physics, many problems in acoustics, finance, biology, engineering, viscoelasticity, hydrology, analysis of dynamic systems, where the evolution of states is influenced by both local changes and historical interactions, and so on [5, 11, 6, 12, 9].

One of the key challenges in solving integro-differential equations lies in their inherent complexity, as traditional methods for solving ordinary differential equations may not be directly applicable. In the last decades, several techniques have been presented to successfully used to approximate different kinds of singular integral equations, such as Jacobi and B-spline collocation method, Crank–Nicolson finite difference method, Daubechies wavelet, Hermite wavelet method, wavelet methods, trigonometric Hermit wavelet, discrete collocation method, Legendre wavelet and Legendre multi-wavelet methods and Petrov-Galerkin method with a wide range of applications, Block boundary value methods, operational matrix-based schemes with relaxation processes [4, 10, 13, 7, 2, 8]. The significance of integro-differential equations is further underscored by their ability to model phenomena that cannot be adequately described by either differentials or integrals alone, thus

offering a more comprehensive framework for understanding complex systems wherein time delays or memory effects play a critical role.

2 Mathematical formulation

The integral equations frequently appear in many fields of mathematics such as game theory, control theory, and numerical analysis. Also, they appear in real physical world problems in other fields of science like as fluid dynamics, queuing theory, filtration theory, electromagnetic, chemical kinetics, laminar boundary-layer theory, solid state physics, plasma physics, the diffusion of neutrons in nuclear reactor dynamics, and so on [5, 11, 6, 12, 9, 1].

In this work, we use the finite element method (FEM) to solve mixed singular integro-differential equation (MSIDE), as follows:

$$\begin{aligned} -u''(x) + f_1(x)u'(x) + f_2(x)u(x) =& f_3(x) + \int_a^x \frac{K_1(x,t)u(t)}{(x-t)^\alpha}dt \\ &+ \int_a^b \frac{K_2(x,t)u(t)}{(x-t)^\beta}dt, \end{aligned} \tag{1}$$

with

$$u(a) = 0, \quad u(b) = 0, \quad \Omega = [a,b] \subset \mathbb{R}, \tag{2}$$

where $K_1(x,t)$, $K_2(x,t)$, and $f_i(x)$, $\quad i = 1,2,3$ are known continuous functions belong to $C^1(\Omega)$, $u(x)$ is the unknown function to be determined, and $\alpha = \beta = \frac{1}{2}$.

The major goal of this research is to apply Lagrange polynomials combined with FEM for solving MSIDE of (1)–(2) and obtain an approximate solution. First, we obtain the weak and variational form of (1). In section 3, we analyze the application and prove the bilinear form is a $V-$ellipticity and continuous. Also, we proved that (1) has a unique solution. By using some theorem and lemma we calculated the order of convergence is $O(h^2)$ in section 4. We present some numerical test examples in section 5. Finally, the conclusions are highlighted in section 6.

3 Finite element method

One of the best techniques for numerically resolving differential equations in structural analysis, electromagnetic potential, fluid flow, ferroelectric, and electromagnetics in engineering and boundary value problems, algebraic equations, complex mathematical problems, and heat transfer, in mathematical modeling, began in the mid-1950s, used to compute such approximations nominated as FEM [1].

First, we obtain the virtual work (or weak form) and variational form of (1). For this purpose, we assume a Sobolev space of $V = H_0^1(\Omega)$, with the following norm:

$$||u||_V^2 = ||u||_{L^2(\Omega)}^2 + ||u'||_{L^2(\Omega)}^2.$$

Also, the bilinear form is $B : V \times V \to \mathbb{R}$; linear functional has a $L : V \to \mathbb{R}$; and

$$B(u, v) = L(v) = \int_\Omega f_3(x)v(x)dx, \tag{3}$$

for all $v(x) \in V$ is an arbitrary function. In addition,

$$\begin{aligned} B(u, v) = &\int_\Omega f_2(x)u(x)v(x)dx + \int_\Omega u'(x)\left(f_1(x)\,v(x) + v'(x)\right)dx \\ &- \int_\Omega v(x)\left(\int_a^x \frac{K_1(x,t)\,u(t)}{(x-t)^\alpha}dt\right)dx \\ &- \int_\Omega v(x)\left(\int_a^b \frac{K_2(x,t)\,u(t)}{(x-t)^\beta}dt\right)dx. \end{aligned} \tag{4}$$

Since we have

$$\begin{aligned} B(\eta_1 u + \eta_2 w, v) = &\int_\Omega \big(\eta_1 u'(x) + \eta_2 w'(x)\big)v'(x)dx \\ &+ \int_\Omega f_1(x)\left(\eta_1 u'(x) + \eta_2 w'(x)\right)v(x)dx \\ &+ \int_\Omega f_2(x)\left(\eta_1 u(x) + \eta_2 w(x)\right)v(x)dx \\ &- \int_\Omega v(x)\int_a^x \frac{K_1(x,t)\left(\eta_1 u(x) + \eta_2 w(x)\right)}{(x-t)^\alpha}dtdx \\ &- \int_\Omega v(x)\int_a^b \frac{K_2(x,t)\left(\eta_1 u(x) + \eta_2 w(x)\right)}{(x-t)^\alpha}dtdx \end{aligned}$$

$$=\eta_1 B(u,v)+\eta_2 B(w,v),$$

then, B is a bilinear form. In this work, we use the linear B-spline (LBS) function as the basis functions of subspace $V_h = \text{span}\{\phi_1, \phi_2, \ldots, \phi_n\}$. If $a = x_0 < x_1 < \cdots < x_n = b$ is a grid with $n+1$ points in the interval $[a,b]$, where $x_i = ih$ for $i = 1, \ldots, n$, and $\Delta x = h = \frac{1}{n}$, then, for $i = 1, \ldots, n$, the LBS is defined as

$$\phi_i(x) = \frac{1}{h}\begin{cases} (x - x_{i-1}), & x \in [x_{i-1}, x_i], \\ (x_{i+1} - x), & x \in [x_i, x_{i+1}], \\ 0, & \text{otherwise.} \end{cases} \tag{5}$$

Thus $\phi_i(x_i) = 1, \phi_i(x_j) = \delta_{ij}$, for $i, j = 1, 2, \ldots, n$, and the value of ϕ in the other nodes is equal to zero. Therefore, we approximate $u_h(x)$ and $v_h(x)$ as

$$u_h(x) = \sum_{i=1}^{n} a_i \phi_i(x), \qquad v_h(x) = \phi_j(x). \tag{6}$$

By the combination of (6) and variational formulation of the problem, we have

$$\begin{aligned} \int_\Omega f(x)\phi_j(x)dx = \sum_{i=1}^{n} a_i \Bigg\{ & \int_\Omega f_2(x)\phi_i(x)\phi_j(x)dx \\ & + \int_\Omega \phi_i'(x)\left(\phi_j'(x) + f_1(x)\phi_j(x)\right)dx \\ & - \int_\Omega \phi_j(x)\left(\int_a^x \frac{K_1(x,t)}{(x-t)^\alpha}\,\phi_i(t)\,dt\right)dx \\ & - \int_\Omega \phi_j(x)\left(\int_a^b \frac{K_2(x,t)}{(x-t)^\beta}\,\phi_i(t)\,dt\right)dx \Bigg\}. \end{aligned} \tag{7}$$

Now, we define

$$\begin{aligned} C_{i,j} = & \int_\Omega \phi_i'(x)\left(\phi_j'(x) + f_1(x)\phi_j(x)\right)dx + \int_\Omega f_2(x)\phi_i(x)\phi_j(x)dx \\ & - \int_\Omega \phi_j(x)\left(\int_a^x \frac{K_1(x,t)}{(x-t)^\alpha}\,\phi_i(t)\,dt\right)dx \\ & - \int_\Omega \phi_j(x)\left(\int_a^b \frac{K_2(x,t)}{(x-t)^\beta}\,\phi_i(t)\,dt\right)dx, \end{aligned} \tag{8}$$

and

$$F_j = \int_\Omega f(x)\phi_j(x)dx. \tag{9}$$

Thus the above system can be expressed as a system of an algebraic equation of the form

$$\sum_{i=1}^{n} C_{ij}a_i = F_j, \quad j = 1, 2, \ldots, n. \tag{10}$$

4 Error analysis

In this section, we aim to establish a lower and upper bound for approximation error. To prove that we need to define the following definition.

Definition 1. The inner product energy can be described as

$$(\cdot,\cdot)_B : V \times V \to \mathbb{R},$$

such that for the Hilbert space V and the $V-$elliptic bilinear form B, we have $(u,v)_B = B(u,v)$. Also, we can define the energy norm as

$$||u||_E^2 = (u,u)_B.$$

Lemma 1. If $f_1(x) \in [M_1, M_2]$, $f_2(x) \in [P_1, P_2]$, and B is a bilinear form defined by (4), then B is continuous.

Proof. First, by (4), we have

$$\begin{aligned} |B(u,v)| = \Bigg| & \int_\Omega f_2(x)u(x)v(x)dx + \int_\Omega u'(x)\left(v'(x) + f_1(x)v(x)\right)dx \\ & - \int_\Omega v(x)\left(\int_a^x \frac{K_1(x,t)\,u(t)}{(x-t)^\alpha}dt\right)dx \\ & - \int_\Omega v(x)\left(\int_a^b \frac{K_2(x,t)\,u(t)}{(x-t)^\beta}dt\right)dx\Bigg|. \end{aligned} \tag{11}$$

In (11) by applying the Sobolev norm and the Cauchy–Schwarz inequality, we have

$$\begin{aligned} |B(u,v)| \leq & \, ||u||_{H^1}||v||_{H^1} + P_2\,||u||_{H^1}||v||_{H^1} + M_2\,||u||_{H^1}||v||_{H^1} \\ & + K_1\left|\int_a^b v(x)\int_a^x \frac{u(t)}{(x-t)^\alpha}dtdx\right| \end{aligned}$$

$$
\begin{aligned}
&+ K_2 \left| \int_a^b v(x) \int_a^b \frac{u(t)}{(x-t)^{\beta}} dt dx \right| \\
&= \left(1 + P_2 + M_2\right) ||u||_{H^1} ||v||_{H^1} \\
&+ K_1 \left| \int_a^b v(x) u(\eta_x) \int_a^x \frac{1}{(x-t)^{\alpha}} dt dx \right| \\
&+ K_2 \left| \int_a^b v(x) u(\zeta_x) \int_a^b \frac{1}{(x-t)^{\beta}} dt dx \right| \\
&\leq \left(1 + P_2 + M_2\right) ||u||_{H^1} ||v||_{H^1} \\
&+ K_1 \left| \int_a^b v(x) u(\eta_x) \frac{1}{1-\alpha} (x-t)^{1-\alpha} \, |_{t=a}^{t=x} \, dx \right| \\
&+ K_2 \left| \int_a^b v(x) u(\zeta_x) \frac{1}{1-\beta} (x-t)^{1-\beta} \, |_{t=a}^{t=b} \, dx \right| \\
&\leq \left(1 + P_2 + M_2\right) ||u||_{H^1} ||v||_{H^1} \\
&+ \frac{K_1 (b-a)^{1-\alpha}}{1-\alpha} \left| \int_a^b v(x) u(\eta_x) dx \right| \\
&+ \frac{K_2 (b-a)^{1-\beta}}{1-\beta} \left| \int_a^b v(x) u(\eta_x) dx \right| \\
&\leq \left(1 + P_2 + M_2 + \frac{K_1 (b-a)^{1-\alpha}}{1-\alpha} + \frac{K_2 (b-a)^{1-\beta}}{1-\beta}\right) ||u||_{H^1} \, ||v||_{H^1},
\end{aligned}
$$

where

$$K_1 = \max |K_1(x,t)|, \quad a \leq x \leq b, \quad a \leq t \leq x$$

and

$$K_2 = \max |K_2(x,t)|, \quad a \leq x \leq b, \quad a \leq t \leq x.$$

Thus B is continuous. □

In addition to the hypothesis of Lemma 1, suppose $T_2 = \max_{a \leq x \leq b} |f_1^{'}(x)|$. Now, we consider the $V-$ ellipticity of B. By using (4) and Lemma 1, we write

$$
\begin{aligned}
\int_{\Omega} f_1(x) v'(x) v(x) dx &= \frac{-1}{2} \int_a^b f_1'(x) (v(x))^2 dx \\
&\geq \frac{-T_2}{2} \int_a^b (v(x))^2 dx
\end{aligned}
$$

$$\geq \frac{-T_2}{2}||v||^2_{H^1}, \tag{12}$$

and

$$\int_\Omega v'(x)v'(x)dx + \int_\Omega f_2(x)v(x)v(x)dx \geq \int_\Omega v'^2(x)dx \geq \frac{1}{1+c}||v||^2_{H^1}. \tag{13}$$

Thus

$$\begin{aligned} B(v,v) &= \int_\Omega v'(x)v'(x)dx + \int_\Omega f_1(x)v'(x)v(x)dx + \int_\Omega f_2(x)v(x)v(x)dx \\ &\quad - \int_\Omega v(x)\int_a^x \frac{K_1(x,t)v(t)}{(x-t)^\alpha}dtdx - \int_\Omega v(x)\int_a^b \frac{K_2(x,t)v(t)}{(x-t)^\beta}dtdx \\ &\geq \left(\frac{1}{1+c} - \frac{T_2}{2}\right)||v||^2_{H^1} - K_1\left(\frac{(b-a)^{1-\alpha}}{1-\alpha}\right)||v||^2_{H^1} \\ &\quad - K_2\left(\frac{(b-a)^{1-\beta}}{1-\beta}\right)||v||^2_{H^1} \\ &= \eta\ ||v||^2_{H^1(\Omega)}, \end{aligned} \tag{14}$$

so

$$B(v,v) \geq \eta\ ||v||^2_{L_2(\Omega)}, \tag{15}$$

where

$$\eta = \frac{1}{1+c} - K_2\left(\frac{(b-a)^{1-\beta}}{1-\beta}\right) - \frac{T_2}{2} - K_1\left(\frac{(b-a)^{1-\alpha}}{1-\alpha}\right),$$

where c is Poincaré's constant. Then, the following lemma can be expressed.

Lemma 2. If $\eta > 0$, then B is $V-$ellipticity.

By applying the Lax–Milgram theorem and Lemmas 1 and 2, the equation (1) has a unique solution.

Since for each particular $\tilde{v}_h$ in V_h, $\inf||u-v_h||_V \leq ||u-\tilde{v}_h||_V$, thus for seeking of an upper bound $u-u_h$, we can take $\tilde{v}_h$ equal to $\tilde{u}_h$. Then

$$||u-u_h||_V \leq c||u-\tilde{u}_h||_V.$$

By using Cea's lemma [3] and

$$||u-u_h||_E = \min_{v_h \in V_h} ||u-v_h||_E$$

for each particular $\tilde{v}_h$ in V_h, we have

$$\alpha||u-u_h||_V^2 \leq B(u-u_h, u-u_h) = ||u-u_h||_E^2. \tag{16}$$

Thus $||u-u_h||_V \leq \frac{1}{\sqrt{\alpha}}||u-u_h||_E$. Also,

$$||u-v_h||_E^2 = B(u-v_h, u-v_h) \leq C||u-v_h||_V||u-v_h||_V. \tag{17}$$

Therefore $||u-v_h||_E \leq \sqrt{C}||u-v_h||_V$. By (16) and (17),

$$||u-u_h||_V \leq \sqrt{\frac{C}{\alpha}} \min_{v_h \in V_h} ||u-v_h||_V. \tag{18}$$

If we define interpolation error $E(x) = u(x) - \tilde{u}_h(x)$, such that error on Ω_e, then

$$E(x_1^{(e)}) = E(x_2^{(e)}) = E(x_3^{(e)}) = 0.$$

Also, by using Rolle's theorem, we have

$$E'(\xi_1) = 0 \qquad \xi_1 \in \left(x_1^{(e)}, x_2^{(e)}\right),$$

$$E'(\xi_2) = 0 \qquad \xi_2 \in \left(x_2^{(e)}, x_3^{(e)}\right),$$

$$E''(\eta) = 0 \qquad \eta \in \left(x_1^{(e)}, x_3^{(e)}\right).$$

We know the polynomial interpolation that we used in our equation, is a piecewise quadratic polynomial. Thus

$$|E''(x)| = u''(x) - u''_h(x) = \int_\eta^x E'''(t)dt = \left|\int_\eta^x u'''(t)dt\right|$$
$$\leq \int_\eta^x |u'''(t)|dt \leq \int_{x_1^{(e)}}^{x_3^{(e)}} |u'''(t)|dt \leq ||1||_{L^2}||u'''||_{L^2},$$

or

$$|E''(x)| \leq h^{\frac{1}{2}}|u|_{H^3(\Omega_e)}.$$

Then

$$\int_{\Omega_e} |E''(x)|^2 dx \leq h|u|^2_{H^3(\Omega_e)} \int_{\Omega_e} dx.$$

Thus

$$||E''||^2_{L^2(\Omega_e)} = |E|^2_{H^2(\Omega_e)} \leq h^2 |u|^2_{H^3(\Omega_e)}.$$

Therefore,

$$\begin{aligned} ||E''||^2_{L^2(\Omega)} = |E|^2_{H^2(\Omega)} &= \int_\Omega |E''(x)|^2 dx = \sum_{e=1}^{M} \int_{\Omega_e} |E''(x)|^2 dx = \sum_{e=1}^{M} |E|^2_{H^2(\Omega_e)} \\ &\leq h^2 \sum_{e=1}^{M} |u|^2_{H^3(\Omega_e)} = h^2 \sum_{e=1}^{M} \int_{\Omega_e} (u'''(x))^2 dx \\ &= h^2 \int_\Omega |u'''(x)|^2 dx = h^2 |u|^2_{H^3(\Omega)}, \end{aligned}$$

that is,

$$|E(x)|_{H^2(\Omega)} \leq h |u|_{H^3(\Omega)}. \tag{19}$$

Similarly, we have

$$|E|^2_{H^1(\Omega)} \leq h^2 |E|^2_{H^2(\Omega)}, \tag{20}$$

that is,

$$||E||_{L^2(\Omega)} \leq h \, |E|_{H^1(\Omega)}. \tag{21}$$

By (19), (20) and (21), we have

$$||E||^2_{L^2(\Omega)} \leq h^2 h^2 h^2 |u|^2_{H^3(\Omega)} = h^6 |u|^2_{H^3(\Omega)}. \tag{22}$$

By using the Sobolev norm, we have

$$\begin{aligned} ||E||^2_{H^1(\Omega)} = ||E||^2_{L^2(\Omega)} + ||E'||^2_{L^2(\Omega)} &\leq h^6 |u|^2_{H^3(\Omega)} + |E|^2_{H^1(\Omega)} \\ &\leq h^6 |u|^2_{H^3(\Omega)} + h^4 |u|^2_{H^3(\Omega)} \leq 2h^4 |u|^2_{H^3(\Omega)}. \end{aligned} \tag{23}$$

Thus the upper bound for the interpolation error as

$$||E||_{H^1(\Omega)} \leq \sqrt{2} h^2 |u|_{H^3(\Omega)}.$$

The unique solution to the variational form is known. Therefore $|u|_{H^2(\Omega)}$ is a constant number. Also, according to (18), if α is the V-ellipticity constant

and C is the continuity constant, then

$$||u - u_h||_V \leq \frac{C}{\alpha}||u - \tilde{u}_h||_V.$$

Thus

$$||u - u_h||_{H^1(\Omega)} \leq \frac{C}{\alpha}\sqrt{2}h^2|u|_{H^3(\Omega)}.$$

Since $|u|_{H^3(\Omega)}$ is constant, and $h \to 0$, thus the method is convergence, and the rate of method is $O(h^2)$.

5 Numerical examples

In this section, we present two examples: one of MSIDE and another singular Volterra integro-differential equation (SVIDE). We compare numerical and accurate solutions of our method with FEM and radial basis function (RBF) methods in tables and figures. Also, we compute the error of examples shown in the Figures, and the accuracy of the method is shown for all examples. Also, we define the root mean square (RMS) or total error, as

$$RMS = \sqrt{\frac{1}{M}\sum_{i=1}^{M}\left(p(t_i)^{exact} - p(t_i)^{numerical}\right)^2},$$

where the total error is RMS and the total number of estimated values is $M = 5$.

In addition, to define the sequence of approximating functions $\{u_i\}_{i\in\mathbb{N}}$, the initial function $u_0 \in C([0,1])$ can be chosen arbitrarily. The following algorithm, based on the method presented in section 3, has been used to solve Examples 1 and 2.

Algorithm 4.1 Step 1. Make the boundary conditions homogeneous
Step 2. Input $n, [a, b]$
Step 3. Set $h = \frac{b-a}{n}$
Step 4. Obtain the virtual work (or weak form) and variational form of (1).
Step 5. For $i = 1$ to n, $x_i = a + ih$, and $\phi_i(x)$ is computed form (5).
Step 6. Compute $u_h(x), v_h(x)$ from (6) for the assumed point.
Step 7. Compute $C_{i,j}$ from (8).

Step 8. Product matrices F_j from (9).
Step 9. Solving (10), obtain an approximate solution of (1).

All results are computed by using Maple and a Lenovo Laptop (Legion Y545) to run the programs. Finally, the RMS of Examples 1 and 2 is given in the last line of the tables.

Example 1. Consider the MSIDE and $0 \leq x \leq 1$ as follows:

$$\begin{aligned} &- u''(x) + e^x u'(x) + x\, u(x) - \int_0^x \frac{1}{\sqrt{x-t}} u(t)dt \\ &- \int_0^1 \frac{1}{\sqrt{x-t}} u(t)dt - f(x) = 0, \end{aligned}$$

where the exact solution $u(x) = 3x^4 - x$, and

$$\begin{aligned} f(x) = &- 37\, x^2 + 12\, \mathrm{e}^x x^3 - \mathrm{e}^x + 3\, x^5 - \frac{512\, x^{\frac{9}{2}}}{105} + \frac{8}{3}\, x^{\frac{3}{2}} - \frac{4}{7}\sqrt{x-1}\,(x) \\ &+ \frac{32\sqrt{x-1}x^2}{35} + \frac{128\sqrt{x-1}x^3}{105} + \frac{256\sqrt{x-1}x^4}{105}. \end{aligned}$$

The inhomogeneous conditions must be transformed into homogeneous boundary conditions via transformation formulas. Comparison of numerical and accurate solutions by our method with FEM and RBF methods are shown in Table 1 and Figure 1. Also, we compute the error of Example 1 in Figure 2.

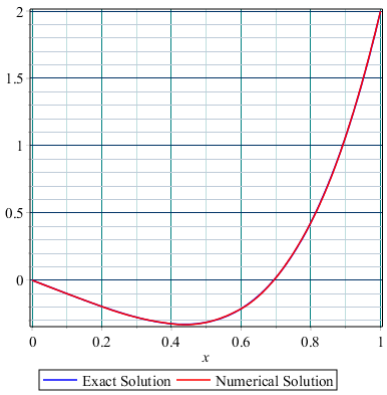

Figure 1: Graph of exact and numerical solutions for Example 1.

Table 1: The result obtain for Example 1.

x	$Exact$	$FEMMethod$	$RBFMethod$	$Cheb-FEMMethod$
0.1	-0.0997000	-0.0998079	-0.0982779	-0.1003080
0.2	-0.1952000	-0.1952376	-0.1936725	$-.19516122$
0.3	-0.2757000	-0.2759063	-0.2740468	$-.27504775$
0.4	-0.3232000	-0.3232568	-0.3214751	-0.3224741
0.5	-0.3125000	-0.3128260	-0.310652	-0.31219453
0.6	-0.2112000	-0.2112657	-0.2093563	-0.2114496
0.7	0.02030000	0.0198278	0.0222087	0.01978290
0.8	0.42880000	0.4287426	0.4306302	0.42852739
0.9	1.06830000	1.0676660	1.0701542	1.0685356
RMS		2.82×10^{-4}	1.66×10^{-3}	4.56×10^{-4}

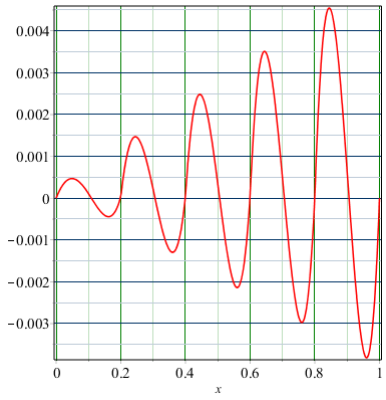

Figure 2: Diagrams of error for Example 1.

Example 2. We assume the SVIDE and $0 \le x \le 1$ as follows:

$$-u''(x)+\sqrt{x}u'(x)+e^x\,u(x)-\int_0^x \frac{1}{\sqrt{x-t}}u(t)dt$$
$$-\int_0^1 \frac{1}{\sqrt{x-t}}u(t)dt-f(x)=0,$$

where the exact solution is a $u(x)=x^3+2\,e^x$, and

$$f(x)=2\,\mathrm{erf}\left(\sqrt{x-1}\right)\sqrt{\pi}\mathrm{e}^x+\frac{1}{35}\left(32\,x^3+16\,x^2+12\,x+10\right)\sqrt{x-1}+3\,x^{5/2}$$

$$-\frac{64x^{7/2}}{35}-4\mathrm{erf}\left(\sqrt{x}\right)\sqrt{\pi}\mathrm{e}^{x}+2\mathrm{e}^{2x}+2\sqrt{x}\mathrm{e}^{x}+\frac{1}{35}\left(35x^{3}-70\right)\mathrm{e}^{x}-6x.$$

First, we convert the boundary conditions at $x = 0$ and $x = 1$ until the example is homogeneous. A comparison between exact and numerical solutions by our method with FEM and RBF methods is shown in Table 2 and Figure 3. Also, we compute the error of Example 2 in Figure 4.

Table 2: The result obtain for Example 2.

x	$Exact$	$FEMMethod$	$RBFMethod$	$Cheb-FEMMethod$
0.1	2.2113418	2.2113258	2.2111969	2.2115616
0.2	2.4508055	2.4507929	2.4507205	2.4507892
0.3	2.7267176	2.7266735	2.7266832	2.7264834
0.4	3.0476493	3.0476138	3.0476679	3.0473934
0.5	3.4224425	3.4223740	3.4225271	3.4223379
0.6	3.8602376	3.8601901	3.8603829	3.8603269
0.7	4.3705054	4.3704358	4.3707312	4.3706852
0.8	4.9630818	4.9630550	4.9633822	4.9631763
0.9	5.6482062	5.6481528	5.6486308	5.6481290
RMS		4.32×10^{-5}	2.06×10^{-4}	1.61×10^{-4}

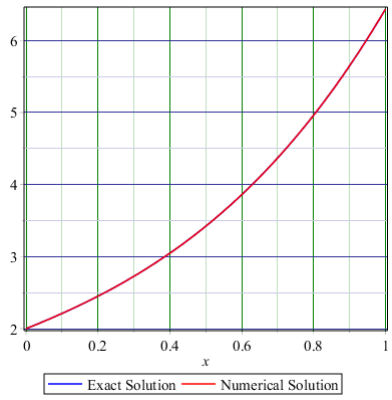

Figure 3: Graph of exact and FEM method for Example 2.

Example 3. We assume the SVIDE and $0 \le x \le 1$ as follows:

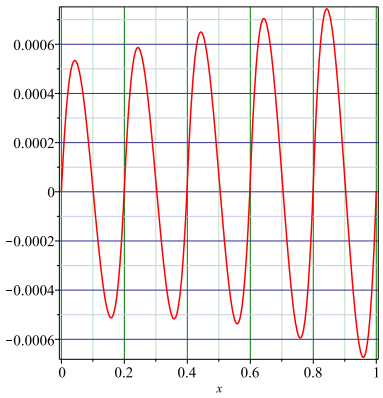

Figure 4: Diagrams of error for Example 2.

$$-u''(x)+x^2u'(x)+2x\,u(x)-\int_0^x\frac{2xt^2}{(x-t)^{\frac{1}{3}}}u(t)dt \\ -\int_0^1\frac{3x^2+t+2}{(x-t)^{\frac{2}{5}}}u(t)dt-f(x)=0,$$

where the exact solution is $u(x)=x^3-x+1$, and

$$\begin{aligned}f(x)=&-4\,x+5\,x^4-3\,x^2-\frac{2187}{2618}x^{\frac{20}{3}}+\frac{243\,x^{\frac{14}{3}}}{220}-\frac{27\,x^{\frac{11}{3}}}{20}-\frac{625}{312}x^{\frac{28}{5}}\\&-\frac{3125}{5382}x^{\frac{23}{5}}+\frac{1675}{936}x^{\frac{18}{5}}-\frac{655}{156}x^{\frac{13}{5}}+\frac{25\,x^{\frac{8}{5}}}{24}-\frac{10}{3}\,x^{\frac{3}{5}}\\&+\frac{10135\,(x-1)^{\frac{3}{5}}\,x^2}{2392}-\frac{10325\,(x-1)^{\frac{3}{5}}\,x^3}{21528}\\&+\frac{38375\,(x-1)^{\frac{3}{5}}\,x^4}{21528}+\frac{625\,(x-1)^{\frac{3}{5}}\,x^5}{312}+\frac{66665\,(x-1)^{\frac{3}{5}}}{21528}\\&-\frac{13775\,(x-1)^{\frac{3}{5}}\,(x)}{21528}.\end{aligned}$$

First, we convert the boundary conditions at $x=0$ and $x=1$ until the example is homogeneous. Comparison between exact and numerical solutions by our method with FEM and RBF method is shown in Table 3 and Figure 5. Also, we compute the error of Example 3 in Figure 6.

Table 3: The result obtain for Example 3.

x	$Exact$	$FEMMethod$	$RBFMethod$	$Cheb-FEMMethod$
0.1	0.9010000	0.9009946	0.8847265	0.9010000
0.2	0.8080000	0.8079910	0.7780601	0.8080000
0.3	0.7270000	0.7269861	0.6861300	0.7270000
0.4	0.6640000	0.6639860	0.6150528	0.6640000
0.5	0.6250000	0.6249798	0.5711002	0.6250000
0.6	0.6160000	0.6159850	0.5607239	0.6160000
0.7	0.6430000	0.6429763	0.5907674	0.6430000
0.8	0.7120000	0.7119892	0.6685135	0.7120000
0.9	0.8290000	0.8289770	0.8020527	0.8290000
RMS		1.52×10^{-5}	3.96×10^{-2}	5.29×10^{-11}

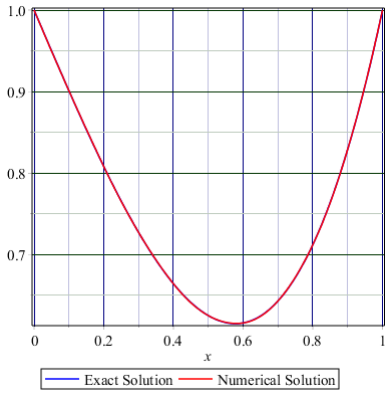

Figure 5: Graph of exact and FEM method for Example 3.

6 Conclusions

In this work, we used the FEM and Lagrange polynomials to solve one of the most important kinds of singular integral equations. The main purpose of this work is to apply Lagrange polynomials and FEM for solving MSIDE (1) and obtain an approximate solution. First, we obtain the weak and variational form of (1), and with the use of the system (10), we can obtain the approximate solution. Then, we proved the convergence of the method. Also, the order of the method is computed. Finally, For efficiency, we presented

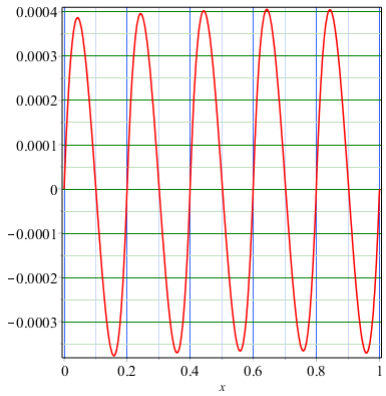

Figure 6: Diagrams of error for Example 3.

some numerical examples and used polynomials of degree 2. Also, the results of comparing between exact FEM method with other methods such as RBF are shown in tables and figures. We conclude the comparison of the results shows that this method has superior accuracy. Also, we computed the error of examples.

References

[1] Ames, W.F. *Nonlinear partial differential equations in engineering*, Academic Press, New York, 1965.

[2] Behera, S. and Saha Ray, S.*An operational matrix based scheme for numerical solutions of nonlinear weakly singular partial integro-differential equations*, Appl. Math. Comput. 367 (2020) 124771.

[3] Brenner, S. and Ridgway Scott. L. *The mathematical theory of finite element methods*, Texts in Applied Mathematics, Springer, 2007.

[4] El-Wakili, S. , Elhanbaly, A. and Abdou, M.A. *Adomian decomposition method for solving fractional nonlinear differential equations*. Appl. Math. Comput, 182 (2006) 313–324.

[5] Liu, H., Ma, Y., Li, H. and Zhang, W. *Combination of discrete technique on graded meshes with barycentric rational interpolation for solving a*

class of time-dependent partial integro-differential equations with weakly singular kernels, Comput. Math. Appl. 141, (2023) 159–169.

[6] Rezazadeh, T. and Najafi, E. *Jacobi collocation method and smoothing transformation for numerical solution of neutral nonlinear weakly singular Fredholm integro-differential equations*, Appl. Numer. Math. 181 (2022) 135–150.

[7] Rosa, M.A., Cuminato, J.A. and McKee, S. *A polynomial collocation method for singular integro-differential equations in weighted spaces*, J. Comput. Appl. Math. 368 (2020) 112526.

[8] Singh, V.K. and Postnikov, E.B. *Operational matrix approach for solution of integro-differential equations arising in theory of anomalous relaxation processes in vicinity of singular point*, Appl. Math. Model. 37(10) (2013) 6609–6616.

[9] Wang, Y.M. and Zhang, Y.J. *A Crank-Nicolson-type compact difference method with the uniform time step for a class of weakly singular parabolic integro-differential equations*, Appl. Numer. Math. 172 (2022) 566–590.

[10] Xu, D. *Numerical solution of partial integro-differential equation with a weakly singular kernel based on Sinc methods,* Math. Comput. Simul. 190 (2021) 140–158.

[11] Zemlyanova, A.Y. and Machina, A. *A new B-spline collocation method for singular integro-differential equations of higher orders*, J. Comput. Appl. Math. 380 (2020) 112949.

[12] Zheng, Z.Y. and Wang, Y.M. *A second-order accurate Crank–Nicolson finite difference method on uniform meshes for nonlinear partial integro-differential equations with weakly singular kernels*, Math. Comput. Simul. 205 (2023) 390–413,

[13] Zhou, Y. and Stynes, M. *Block boundary value methods for solving linear neutral Volterra integro-differential equations with weakly singular kernels*, J. Comput. Appl. Math. 401 (2022) 113747.